

A Performance Controllable Octree Construction Method

Zen Chen, Hong-Long Chou, and Wen-Chao Chen

Department of Computer Science, National Chiao Tung University, Hsinchu, Taiwan
zchen@cs.nctu.edu.tw, hlchou@altek.com.tw, chaody.cs94g@nctu.edu.tw

Abstract

The conventional octree construction method is implemented iteratively at consecutive subdivision levels. The resultant octree models at different subdivision levels contain quite different octant compositions, so the system performance, in terms of model accuracy, memory space and construction time, changes widely with the subdivision level number. Since the big system performance gap is not desirable for the practical application, new construction methods must have a finer control over the system performance. In the paper a new construction method is proposed using new types of octree octants. Interesting properties and computer simulations of the new method are presented. The performance comparison between the conventional method and the new method is made under the comparable XOR projection error condition. It is shown that under this condition the memory space and construction time required by the conventional method can be reduced significantly by the new method.

1. Introduction

The octree construction methods derive the object octree model via the intersection of the viewing volumes generated from the silhouettes [1]-[4]. The resultant octree model can serve as a bounding volume of the real object. Other methods like the voxel coloring methods and the visual hull methods also attempt to construct the object geometry from the silhouettes [5]-[6]. The conventional octree construction methods are implemented iteratively at consecutive integer subdivision levels. There are wide variations in the system performance in terms of memory accuracy, memory space, and construction time. Since the big system performance gap is not acceptable in the practical application, new

construction methods must have a finer control over the system performance. Chou and Chen [4] developed such a method to control the reconstructed model accuracy via the XOR image error between the binary projection image of the constructed octree model and the real object silhouette. In this method the traditional grey octant is divided into grey-grey octant and grey-black octant, depending on if the XOR back-projection error of the grey octant is less than a pre-specified XOR error upper bound. The classified grey-black octant is treated as a black octant and will not be further subdivided. They used the experimental results to show that under the comparable XOR projection error condition the memory space and construction time required by the conventional method can be reduced by their developed method. However, due to the constraint that the resultant octree model must be a bounding volume of the original object, the memory and construction time reductions by the method are only to a certain extent.

In the paper the restriction imposed on the constructed octree model is lifted in order to push the memory and construction time reductions to a greater extent. The design detail of the new method and its properties will be described. Experimental results on the simple and complex objects are used to give more insight into the new method.

2. Design of a new octree construction method

In the conventional octree construction method the type of an octant is classified by an intersection test between the projected octant image and the real object silhouette in each view. To speed up the intersection test, an octant is approximated by its bounding sphere and the intersection test is executed using precompiled signed distance maps derived from the object silhouettes [1]. The signed distance map for each silhouette view is generated in advance using a

distance definition (the chess board distance in this case). The distance value at the circle center c of the bounding circle of a projected octant image is denoted by $DistMap(c)$. The radius r of the bounding circle of the octant projected image is compared with $DistMap(c)$ to determine the intersection relationship. Table 1 gives the intersection relationship between the projected octant image and its associated silhouette.

Table 1. Intersection relationship between the projected octant image and its associated silhouette

| | | |
|---------------------|-------------------------------------|--|
| $DistMap(c) \geq 0$ | $r > DistMap(c)$ in any view | the projected octant image intersects the silhouette (indicating a grey octant) |
| | $r \leq DistMap(c)$ in all views | the octant projected image is within the silhouette (indicating a black octant) |
| $DistMap(c) < 0$ | $r > -DistMap(c)$ in any view | the octant projected image intersects the silhouette (indicating a grey octant) |
| | $r \leq -DistMap(c)$ in any view | the octant projected image is outside the silhouette (indicating a white octant) |

To measure the accuracy of the constructed model, we compute the exclusive OR (XOR) between the binary silhouette image $S_{v,C}$ of the constructed object C and the true object silhouette $S_{v,T}$ for all views ($v=1, \dots, N-1$). The model accuracy is the average of the XOR projection errors across all the views:

$$XOR \text{ error} = \frac{1}{N} \sum_{v=1}^N S_{v,C} - S_{v,T}.$$

The pre-specified XOR projection error upper bound is denoted by P . There are five types of octants at each subdivision level l in the new method: $B_{l,N}$ (black), $W_{l,N}$ (white), $GB_{l,N}$ (grey-black), $GW_{l,N}$ (grey-white), and $GG_{l,N}$ (grey-grey). The black and white octants are the same as in the conventional method and the new types of grey octants are defined below:

A conventional grey octant at level l is called a grey-white ($GW_{l,N}$) octant if its bounding circle circle c has a negative distance value, $DistMap(c) < 0$ and the black extent of the octant satisfies the condition: $0 < r + DistMap(c) \leq P$ in any particular view $v \in [1, N]$.

A conventional grey octant at level l is called a grey-black ($GB_{l,N}$) octant if its bounding circle c has a non-negative distance, $DistMap(c) \geq 0$ and the white extent of the octant satisfies the condition: $0 < r - DistMap(c) \leq P$ in all views $v \in [1, N]$.

If a grey octant cannot be defined as one of the above two, it is called a grey-grey ($GG_{l,N}$) octant. That is, a $GG_{l,N}$ octant is one whose white and black extents exceed the projection error bound P both.

With the new definition of the grey octant types the

octant subdivision scheme of the new construction method is modified as follows:

At each level $l = 0, 1, \dots, L_{N,P}$ only the $GG_{l,N}$ octants need to be subdivided into eight child octants. The octant subdivision process is performed iteratively from level to level until there are no new $GG_{l,N}$ octants at the next (finer) level.

Definition:

The final level of the new method with a specified XOR projection error bound P , $L_{N,P}$, is defined as the level at which the set of grey-grey octants generated by the new method is empty.

3. Properties and system performance analysis of the new construction method

In the following the notation $GG_{l,C}$ stands for a grey-grey octant generated at level l in the conventional method or the set of all grey-grey octant generated at level l , judged from the context. The corresponding notation is $GG_{l,N}$ for the new method. The notations for other octants are similarly defined.

From the experiments reported below, one often finds a common octant subdivision pattern as follows. Starting from the root octant at level 0, eight or less grey sub-octants are generated at level 1. The new grey octants generated are recursively subdivided. When the level is sufficiently large (e. g. level > 4) any grey octant will be generally subdivided into 4 grey, 2 black and 2 white child octants. This pattern is called the 4-2-2 (octant) subdivision pattern hereafter.

Definition:

The (object) octree memory space of the conventional method is defined to be the space to store the sets of black octants at all levels and the set of grey octants at the final level. The (logical) object construction time of the conventional method is defined to be the total number of octants generated by conventional method at all levels. (This total octant number determines the actual octree construction time.)

It is difficult to derive the precise object memory size and the object octree construction time of the three construction methods, but it is desirable to have a rule of thumb for calculating these figures for performance evaluation. A basic observation made here is the 4-2-2 subdivision pattern in the conventional method, as illustrated below.

In the following some interesting properties of the conventional and new octree construction methods will be given without proof due to space limitation.

Property 1:

In the conventional method when the final subdivision level is sufficiently large, both the octree memory space and construction time increase

approximately four times as the level increases by one.

Property 2:

In the conventional method when the final subdivision level becomes sufficiently large the XOR projection error reduces roughly by half as the level increases by one.

To roughly estimate the XOR error of the conventional method, let the minimum and maximum bounding circle diameters of all octant projected images at level l be denoted by $[D_{\min,l}, D_{\max,l}]$. These values at each level indicate roughly the minimum and maximum projection errors of the grey octants obtained by the conventional method. They will be used to specify the XOR projection error upper bound parameter P of the new construction method.

Definition:

The XOR error of the new method specified by a value P in the interval $[P_a, P_b]$ is said to be comparable to that of conventional method specified by level L_C if the XOR error of the new method for the particular value P has a closer distance to XOR_{L_C} than it does with XOR_{L_C-1} or XOR_{L_C+1} . And the interval $[P_a, P_b]$ is the comparable XOR interval corresponding to the conventional level L_C .

Definition:

The object memory space of the new method is defined as the space to store the set of black octants and the set of grey-black octants at all levels generated in the method. The object construction time of the new method is defined to be the total number of all five kinds of octants generated at all levels in the method.

Property 3:

The final subdivision level of the new method associated with a specified XOR error bound P is generally given by $L_{N,P} = L_C - 1$ when $P = D_{\min,L_C}$, and $L_{N,P} = L_C - 2$, when $P = D_{\max,L_C}$.

Property 4:

Under the compatible XOR error condition the ratio of the object memory size of the conventional method to that of the new method, $M_{C,L_C} / M_{N,P}$, is roughly in the interval of $[10, 80]$. Similarly, the ratio of the object construction time of the conventional method to that of the new method, $T_{C,L_C} / T_{N,P}$, is roughly in the interval $[10, 40]$.

From above the new method has a much better memory and time compression ratios than the conventional method under the comparable XOR error condition. This is mainly due to the introduction of the new octant type of grey-white and grey-black octants so that the object model constructed is no longer a bounding volume of the real object. However, there is a price to pay for the performance improvement. That is, when the XOR projection bound P is greater than

the half size of the most elongated part (i.e., the finest details) in the object model, then it is possible that the constructed object model obtained by the new method may have a missing part.

4. Experimental results

We test our method on a variety of synthetic and real objects of different geometric complexity.

Experiment 1: In this experiment 10 images of a toy dinosaur resting on a turntable are taken. Each image has a resolution of 2700 x 1800 pixels.

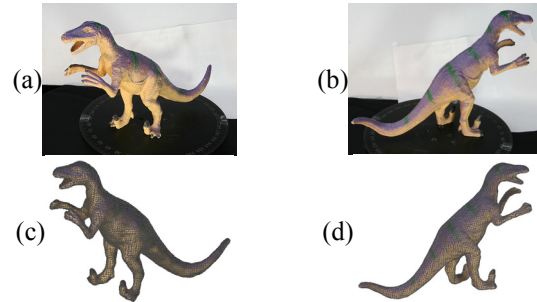


Fig. 1. (a)-(b) Two sample original dinosaur images. (c)-(d) Reconstructed dinosaur model represented in a mesh network with the texture mapping.

The camera projection matrix is used to compute the ranges of the minimum and maximum diameters at each possible subdivision level. They are given in Table 2.

Table 2. The diameter ranges of the bounding circles of the projected octant images at all levels.

| Level | 1 | 2 | 3 | 4 | 5 | 6 | 7 | 8 | 9 | 10 |
|--------------|------|------|-----|-----|-----|----|----|----|----|----|
| $D_{\min,l}$ | 1590 | 698 | 350 | 172 | 90 | 46 | 22 | 12 | 6 | 2 |
| $D_{\max,l}$ | 3176 | 1398 | 676 | 336 | 166 | 80 | 42 | 22 | 12 | 8 |

The main intermediate results of the conventional and new construction methods are collected to show their performances. Table 3 is the tabulation of the numbers of all types of octants generated by the conventional method using $L_C = 8$ and 9 and the new method with the comparable XOR projection error upper bounds $P = 31$ and 15. From this table one can check the important properties of the methods including (i) the relative sizes of the various sets of octants at each level, (ii) the comparable final level numbers, and (iii) the XOR errors at the final levels.

Based on the comparable intervals of P one can compute the memory and construction time compression ratios (CRs) between the conventional and the new methods. In the case of Table 3, the actual memory and time CRs are 52 and 29, respectively, when $P=31$ and 42 and 26 when $P=15$. Fig. 2 shows the memory compression ratio falls in the interval $[10, 80]$ and the time compression ratio falls in the interval

[10, 40] for $P \in [5, 80]$.

Table 3. The statistics of octant numbers and XOR errors for the two construction methods.

| | $L_c=8, XOR=66,228$ | | | | | $P=31, XOR=65,188$ | | | | |
|---|---------------------|----|--------|----|--------|--------------------|------|------|------|------|
| | B | GB | GG | GW | W | B | GB | GG | GW | W |
| 0 | 0 | 0 | 1 | 0 | 0 | 0 | 0 | 1 | 0 | 0 |
| 1 | 0 | 0 | 4 | 0 | 4 | 0 | 0 | 4 | 0 | 4 |
| 2 | 0 | 0 | 14 | 0 | 18 | 0 | 0 | 14 | 0 | 18 |
| 3 | 0 | 0 | 59 | 0 | 53 | 0 | 0 | 42 | 17 | 53 |
| 4 | 0 | 0 | 202 | 0 | 270 | 0 | 0 | 143 | 59 | 134 |
| 5 | 21 | 0 | 800 | 0 | 795 | 21 | 54 | 352 | 359 | 358 |
| 6 | 407 | 0 | 3107 | 0 | 2886 | 109 | 981 | 26 | 1347 | 353 |
| 7 | 3266 | 0 | 12392 | 0 | 9198 | 2 | 201 | 0 | 5 | 0 |
| 8 | 18934 | 0 | 48086 | 0 | 32116 | | | | | |
| 9 | | | | | | | | | | |
| | $L_c=9, XOR=33,852$ | | | | | $P=15, XOR=35,336$ | | | | |
| | B | GB | GG | GW | W | B | GB | GG | GW | W |
| 0 | 0 | 0 | 1 | 0 | 0 | 0 | 0 | 1 | 0 | 0 |
| 1 | 0 | 0 | 4 | 0 | 4 | 0 | 0 | 4 | 0 | 4 |
| 2 | 0 | 0 | 14 | 0 | 18 | 0 | 0 | 14 | 0 | 18 |
| 3 | 0 | 0 | 59 | 0 | 53 | 0 | 0 | 51 | 8 | 53 |
| 4 | 0 | 0 | 202 | 0 | 270 | 0 | 0 | 178 | 24 | 206 |
| 5 | 21 | 0 | 800 | 0 | 795 | 21 | 22 | 586 | 192 | 603 |
| 6 | 407 | 0 | 3107 | 0 | 2886 | 252 | 394 | 1468 | 1157 | 1417 |
| 7 | 3266 | 0 | 12392 | 0 | 9198 | 784 | 4216 | 184 | 5232 | 1328 |
| 8 | 18934 | 0 | 48086 | 0 | 32116 | 18 | 1387 | 0 | 65 | 2 |
| 9 | 88349 | 0 | 182434 | 0 | 113905 | | | | | |

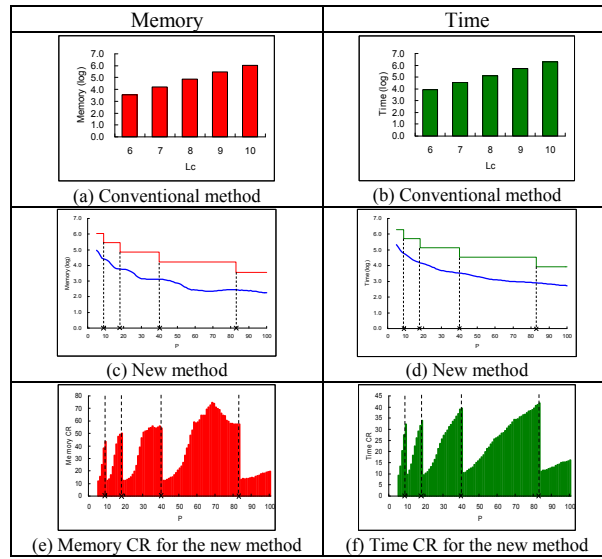


Fig. 2. The plots of the memory spaces and construction time of the conventional and new methods and the compression ratio under the comparable quality condition.

Experiment 2: In Fig. 3 additional synthetic and real objects are used for the octree reconstruction. A proper XOR projection error bound P is used for each object. It is found that the different object geometric complexities have minor effect on the system performance.

5. Conclusions

In the paper a new octree construction method has been presented. The conventional grey octants are refined into grey-grey, grey-black, and grey-white

octants in the new method. The octree model produced by the new method approaches the real object from both object outside and inside, since the grey-black and grey-white octants are generated.

Interesting properties and experimental results show that under the comparable XOR error condition the memory space and construction time required by the conventional method can be reduced by a factor of 10 to 80 and a factor of 10 to 40, respectively, using the new method. However, there is a price to pay for the new method. That is, a fine object part may be missing if the XOR projected error bound P is greater than twice the minimum width of the object part.

Some possible directions for future research are:

- 1) Use of the octree model to solve the point correspondence problem in stereo vision [7]-[8].
- 2) Use of the octree model as the initial approximate object model for dense reconstruction.

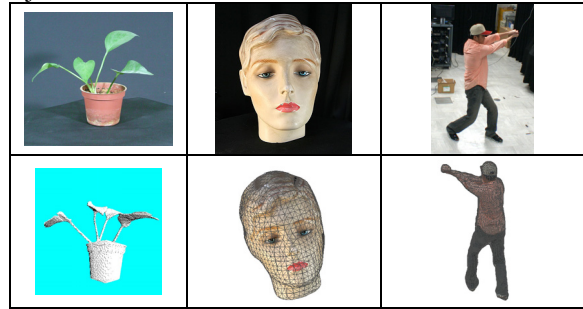


Fig. 3. The sample original images and the constructed textured models

References

- [1] R. Szeliski, "Rapid octree construction from image sequences," *Computer Vision, Graphics and Image Processing: Image Understanding*, vol. 58, no. 1, pp. 23-32, 1993.
- [2] G. K. M. Cheung, T. Kanade, J.Y. Bouguet and M. Holler, "A real time system for robust 3D voxel reconstruction of human motions," in *Proc. IEEE Conf. Computer Vision and Pattern Recognition*, 2000, pp.714-720.
- [3] Y.H. Fang, H.L. Chou, and Z. Chen, "3D shape recovery of complex objects from multiple silhouette images," *Pattern Recognition Letters* 24, 1279-1293, 2003.
- [4] H. L. Chou and Z. Chen, "Fast octree construction endowed with an error bound controlled subdivision scheme," *J. of Information Science and Engineering*, vol. 22, no. 3, pp. 641-657, 2006.
- [5] S. M. Seitz and C. R. Dyer, "Photorealistic scene reconstruction by voxel coloring," *Int. J. of Computer Vision*, Vol. 35, no. 2, pp. 151-173, 1999.
- [6] W. Matusik, C. Buehler, and L. McMillan, "Polyhedral visual hulls for real time rendering," in *Proc. 12th Eurographics Workshop on Rendering*, pp. 115-125, 2001.
- [7] D. Scharstein and R. Szeliski, "A taxonomy and evaluation of dense two-frame stereo correspondence algorithms," *Int. J. Computer Vision*, vol. 47, no. 1, pp. 7-42, 2002.
- [8] Y. Deng, Q. Yang, X. Lin, and X. Tang, "Asymmetric patch-based correspondence model for occlusion handling," in *Proc. IEEE Int. Conf. Computer Vision*, vol. 2, pp. 1316-1322, 2005.